Eur. Phys. J. D **43**, 241–245 (2007)
DOI: 10.1140/epjd/e2007-00114-9

THE EUROPEAN PHYSICAL JOURNAL D

Multiply negatively charged aluminium clusters

Production of Al_n^{2-} in a Penning trap

N. Walsh, F. Martinez, G. Marx, and L. Schweikhard[a]

Institut für Physik, Ernst-Moritz-Arndt-Universität Greifswald, 17487 Greifswald, Germany

Received 11 August 2006 / Received in final form 25 October 2006
Published online 24 May 2007 – © EDP Sciences, Società Italiana di Fisica, Springer-Verlag 2007

Abstract. The first observation of gas-phase aluminium dianions, Al_n^{2-}, is reported. Singly negatively charged aluminium clusters are converted to dianions by exposure to low-energy electrons in a Penning trap. Attachment of such secondary electrons to the monoanions leads to the formation of dianionic clusters, as earlier observed for the noble metals, copper, silver and gold. The present work extends the 'electron-bath technique' to the trivalent aluminium. The observation of Al_n^{2-} as a function of cluster size is compared to estimates of the second electron affinities of Al_n as given by a combination of first electron affinities and the charged conducting-sphere model. This simple approach is found to describe the appearance size (size of smallest Al_n^{2-} observed) very well.

PACS. 36.40.-c Atomic and molecular clusters – 36.40.Wa Charged clusters

1 Introduction

During the last decade much interest has been paid to gas-phase multiply negatively charged ions. Such species can exist only above certain cluster sizes. In addition, whilst singly-charged species are quite straight-forward to produce, the creation of polyanions is complicated by the presence of a Coulomb barrier that hinders the attachment of an electron to a negatively charged species. The Coulomb barrier also enriches the physics of multiply-charged anions, in particular in the case of a species with a negative electron affinity, by providing a potential barrier that inhibits the immediate loss of excess electrons and results in metastability.

To date, experimental and theoretical investigations of aluminium clusters have focused on their electronic [1] and geometric structures [2], as well as on their reactivities with other elements [3]. However, the experimental investigations have been limited to cationic [4–8] and singly negatively charged species [9–12]. Previously at Cluster Trap, the production of dianionic metal clusters composed of the monovalent elements, Au, Ag and Cu [13,14] has been investigated, as well as, more recently, the production of fullerene dianions [15]. These investigations are now extended to trivalent aluminium in the framework of the determination of the cluster properties as a function of both charge-state and size, thus, distinguishing between their electronic and geometric structural aspects [16].

The electron-bath technique is one of many methods developed in the last two decades to produce gas-phase dianionic molecules and clusters. Previously, multiply negatively charged O_2 clusters were observed following the attachment of low-energy electrons to neutral O_2 clusters produced by nozzle expansion [17], dianionic carbon clusters as small as C_7^{2-} were produced by sputtering a graphite target [18] and gas-phase multiply-charged anions composed of more than one element, for example, tetrahalide ions, have been created by electrospray ionisation [19]. In addition metal-cluster dianions were observed following pulsed nitrogen-laser ablation of various metal targets in vacuum [20].

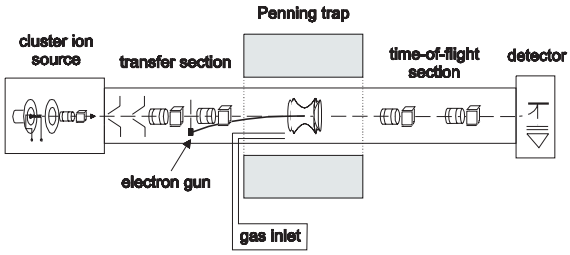

Fig. 1. Overview of the experimental arrangement.

2 Experimental arrangement and procedure

The Cluster Trap apparatus (Fig. 1) [21–23] comprises of a source chamber, a Penning ion trap mounted in the homogeneous region of a superconducting magnet and a section for time-of-flight (ToF) mass analysis.

[a] e-mail: lschweik@physik.uni-greifswald.de

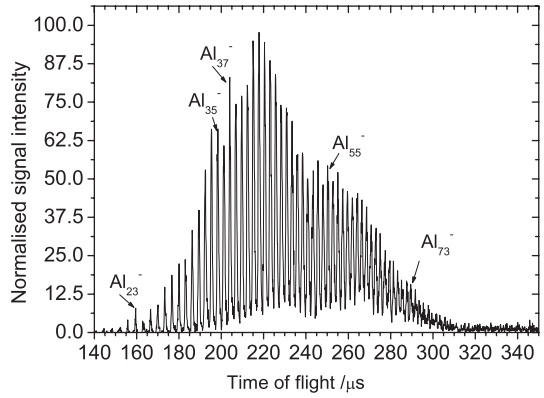

Fig. 2. Al_n^- ToF spectrum after 500 ms storage. $U_T = 13$ V, $p = 1 \times 10^{-6}$ mbar, 3×10^5 ion counts for 600 cycles.

The output of a frequency-doubled Nd:YAG laser, a ns-pulse of a few mJ, is focused to approx. 100 μm to ablate a plasma from the surface of a metal wire into a He gas pulse [24]. As the plasma constituents cool, clusters begin to form. The helium gas subsequently expands adiabatically through a 0.7 mm-nozzle into high vacuum. The laser vaporisation source produces neutral and singly-charged (positive and negative) clusters [24] which are transferred by electrostatic ion-optical elements to a Penning trap [25].

The Penning trap [25] consists of a segmented ring electrode and two end-cap electrodes, all hyperbolical in shape. Radial ion confinement is due to the magnetic field. Axial ion confinement is achieved by application of a static quadrupolar electric field due to a potential difference, U_0, between the ring and end-cap electrodes. The depth of the potential well in the axial direction is $U_T = U_0/2$ (asymptotically-symmetric trap [26]).

In-flight capturing is achieved by lowering the potential on the first end-cap electrode by a few volts and raising it up to the storage value after the ions have entered [27]. Due to the expansion of the helium gas pulse through the nozzle, the clusters leave the source with about the same velocity, but with different energies according to their different masses. The potential, U_{EC}, on the end-cap electrodes and the depth of the capture pulse determine the size-range of clusters that are captured [21]: larger clusters have enough energy to pass through the trap unhindered, whilst clusters that are too small cannot enter the trap at all. Figure 2 shows a typical example of a cluster-ion distribution that was created in the source, transferred to and stored in the Penning trap (without application of additional rf fields that would influence the trapped ion distribution).

Dianions are created by exposure of the stored monoanions to an electron bath [28,29]: low-energy electrons are produced by electron-impact ionisation of argon gas pulsed into the trap region. The ionising (primary) electron beam is emitted from a heated filament situated halfway between the cluster source and the Penning trap (see Fig. 1). It is applied for 0.5 s to 3 s at an energy of approximately 40 eV with respect to the endcap potential, U_{EC}. The axial trapping potential is typically a few up to a few tens of volts (see below). If the stored secondary electrons have sufficient energy to overcome the Coulomb barrier of the monoanions, dianions may form. After a variable reaction period, the ions are axially ejected through the second endcap and pass a ToF drift section for mass analysis. The experimental cycle is repeated a few hundred times to increase the statistical significance of the data.

3 Results and discussion

3.1 Expected dianion appearance sizes

In the charged conducting-sphere model [30], the electron affinity, EA, is given by

$$EA(n,z) = W + \left(z - \frac{1}{2}\right)\frac{1}{4\pi\varepsilon_0}\frac{e^2}{R(n)}, \qquad (1)$$

where W is the bulk work function of the metal, z is the charge state, $R(n) = R_a n^{1/3}$ is the radius of the cluster (containing n atoms) and $R_a = 0.1431$ nm is the atomic radius of aluminium [31]. Note that $EA(n,0)$ is generally called the first electron affinity, $EA1$, while $EA(n,-1)$ is the second electron affinity, $EA2$.

A more accurate estimate of the value of $EA2$ [32–34] can be obtained for clusters by use of existing experimentally determined values of $EA1$ [1,10]. If it is assumed that the values of $EA2$ and $EA1$ differ only by the Coulomb repulsion between the two excess electrons, an estimate for the value of the $EA2$ can be obtained from

$$EA(n,-1) = EA(n,0) - \frac{1}{4\pi\varepsilon_0}\frac{e^2}{R(n)}. \qquad (2)$$

For a dianion, Al_n^{2-} to be stable, the second electron affinity of Al_n has to be positive. As Figure 3 shows, in the case of the charged conducting-sphere model, $EA2$ is positive for $n \geq 45$. If experimentally determined values of $EA1$ [1,10] are taken into account to estimate the values of $EA2$ via equation (2), clusters containing $n \geq 38$ are expected to have positive second electron affinities. However, due to the Coulomb barrier of the monoanions, long-lived dianions may also exist for smaller cluster sizes (that have a negative electron affinity). If the surplus electron has insufficient energy to overcome the Coulomb barrier, it can only detach from the cluster via tunnelling through the barrier. The potential as a function of distance, r, from the center of the cluster is [30]

$$V_C(r,R) = \frac{e^2}{4\pi\epsilon_0}\left(\frac{|z|}{r} - \frac{R^3}{2r^2(r^2-R^2)}\right), \qquad (3)$$

where again, for dianions, $z = -1$. The lifetime of Al_n^{2-} versus electron detachment is plotted in Figure 3b as a function of cluster size. It is estimated [14], by considering the probability that the electron will tunnel through the Coulomb barrier of the monoanion using the WKB

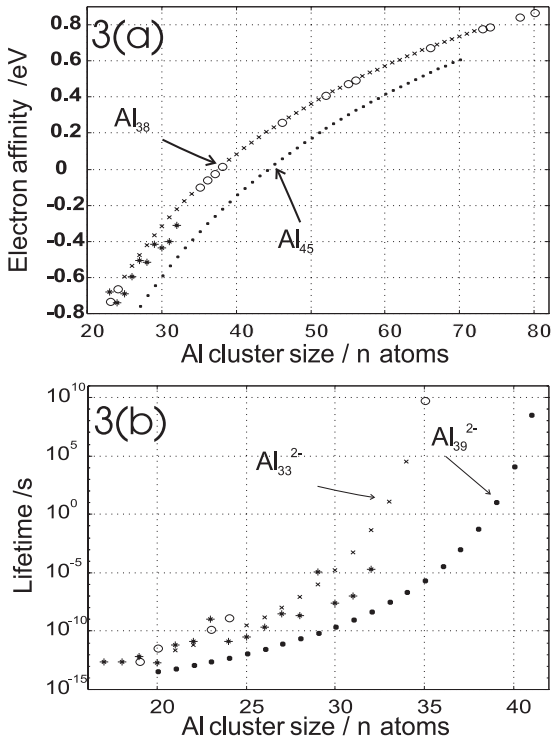

Fig. 3. Estimates of (a) second electron affinities of Al_n and (b) lifetimes of Al_n^{2-} as a function of cluster size. (•) Estimates of $EA2$ using equation (1). (○) $EA2$ estimated using equation (2) and $EA1$ value of [1]. (∗) $EA2$ estimated using equation (2) and $EA1$ values of [10]. (×) $EA2$ estimates using value of $EA1$ obtained by interpolation using experimental values of $EA1$ from publications listed above.

approximation [35]. For $EA2$ values as calculated for the charged conducting-sphere model, aluminium-cluster dianions containing 39 or more atoms are predicted to exist long enough to be observed (for an experimental time of 1 s). If the $EA2$'s are estimated using the experimental $EA1$ values, the lifetimes of clusters as small as Al_{33}^{2-} are longer than 1 s.

3.2 Relative abundance of dianions observed experimentally

Figure 4 shows typical ToF spectra without and after the application of a primary electron beam. For this particular measurement, monoanions, Al_{34}^- to Al_{44}^- were selected by driving out the smaller and the larger clusters by resonant radial rf fields. For Figure 4 (bottom), the cluster ensemble was exposed to the electron beam and thus, to the electron-bath. Dianions, Al_{38}^{2-} and larger, are clearly observed. The size dependence of the relative abundance of dianions (with respect to the sum of mono- and di-anions of a given cluster size) is plotted in Figure 5. As expected and observed earlier for other species [13–15,28,36], the relative abundance of dianions increases as a function of cluster size. In these measurements, it saturates very fast, within only 3 cluster sizes. In the previous section, Al_{33}^{2-}

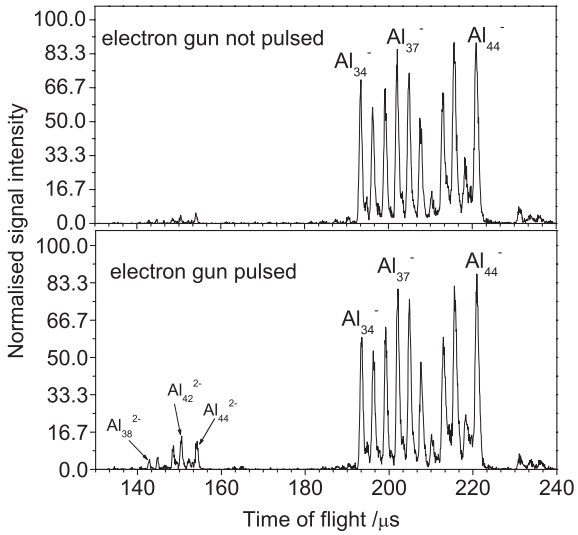

Fig. 4. Top: ToF spectrum of captured and size-range selected aluminium cluster monoanions. Bottom: ToF spectrum where in addition to the above experimental steps, the electron-bath technique has been applied for a reaction time of 1 s at a trapping voltage of $U_T = 13$ V. 3×10^4 ion counts were recorded in 300 additions.

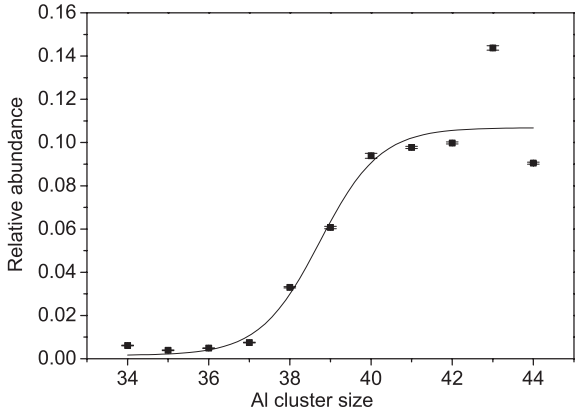

Fig. 5. Relative abundance of Al dianions as a function of cluster size as derived by evaluation of Figure 4 (bottom).

is estimated to be the smallest dianion that should be observed for an experimental time of 1 s. Signals for Al_{38}^{2-} and larger clusters are clearly identified in Figure 4. However, some counts of dianions as small as Al_{34}^{2-} have also been detected.

3.3 Dianion yield as a function of electron bath parameters

The conversion efficiency from mono- to di-anions depends on the particular parameters of each measurement. Figure 6 shows the dianion yield as a function of trapping depth (top) and reaction time (bottom) in the electron-bath. If the trapping depth is too low, there are no electrons with sufficient energy to overcome the Coulomb barrier of the monoanions. Typically, trapping depths in excess of about 5 V are needed for significant dianion

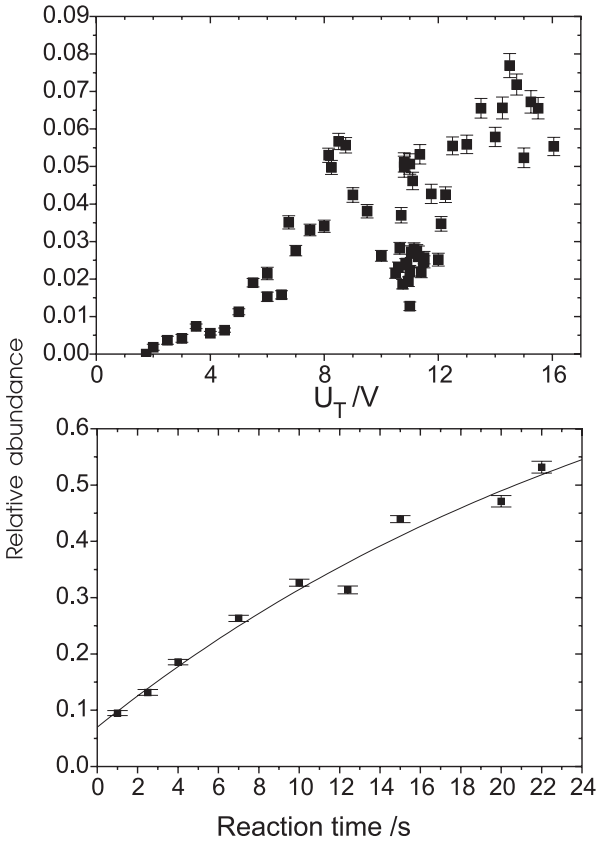

Fig. 6. Top: relative abundance of dianions (Al_{55} to Al_{90}) as a function of trapping depth. Electron beam applied for $T_e = 300$ ms. Reaction time = 1 s. Bottom: relative abundance of dianions (Al_{48} to Al_{84}) as a function of reaction time. $p = 1.4 \times 10^{-6}$ mbar. $T_e = 1$ s.

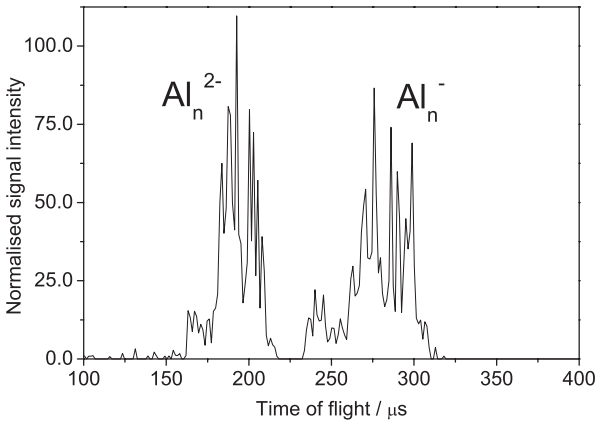

Fig. 7. ToF spectrum depicting dianion yield (Al_{48}^{2-} to Al_{84}^{2-}) for a reaction time of 22 s.

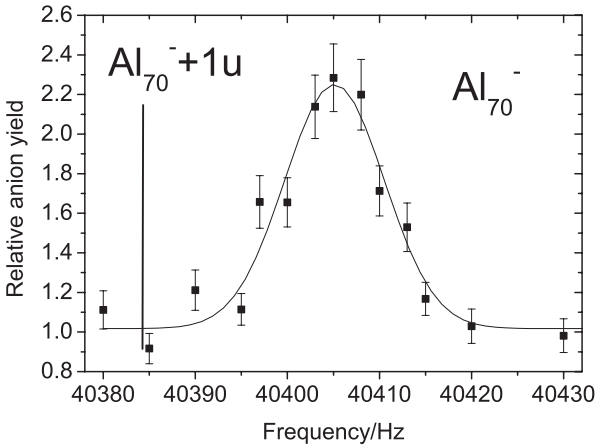

Fig. 8. Relative Al_{70}^- yield (normalised to the counts of Al_{70}^- recorded in a reference cycle where no centering is applied) as a function of the frequency of the applied quadrupolar rf field.

yields. In the region between about $U_T = 10$ V and $U_T = 12$ V a very large "chaotic" fluctuation is observed. Such a behaviour has been reported earlier [37] but is not yet fully understood. It may be due to the conditions of steering the electron beam through the trap. More likely, however, it may reflect a variation in trapping conditions or instabilities in the electron motion (effects dependent on the nature of the simultaneous storage of electrons and monoanions) which in turn influences the likelihood of electron attachment to the monoanions.

After optimisation of the other electron-bath parameters for maximum dianion yield, a series of measurements was performed for reaction times up to 22 seconds (bottom of Fig. 6). A long reaction time between the monoanions and the low-energy electrons in the electron-bath resulted in dianion abundances above 50% (see also the ToF spectrum of Fig. 7). For interaction durations up to 22 seconds, the time dependence seems linear. The results presented here for aluminium-cluster dianions deviate from earlier findings where the dianion yield levelled off after approximately 2–4 seconds and "new" electrons had to be supplied if further dianion creation was intended [14,15]. The quenching of electron attachment was previously explained [37], by transfer of the axial electron motion into cyclotron motion which undergoes relatively fast damping due to radiative cooling. Thus the axial damping time would be given by the equilibration of axial and radial electron motion. As this depends on the density of the electron cloud, it seems that in the present experiments less electrons have been stored. This assumption is still to be tested. However, there is no easy procedure to investigate the electron cloud. In fact, the attachment of electrons to monoanions and thus the formation of dianions has been suggested as a monitor of the electron ensemble [37].

3.4 Quadrupolar excitation resonances as a test of cluster purity

Presently, further experiments are under way where the cluster sizes are investigated one at a time. For the capturing of several ion bunches and for the preparation of the clusters for further studies, the technique of resonant (i.e. applied frequency $\nu_{rf} = \nu_c = qB/m$, the cyclotron frequency for ions of mass m and charge q) quadrupolar-excitation assisted buffer-gas cooling [38,39] is used. As shown in Figure 8 this method significantly enhances the number of precursor ions of interest as compared to

non-resonant frequencies or no such application at all (reference measurements for the relative values of Fig. 8). There is an additional advantage: Note that the ToF detection at Cluster Trap presently allows only a rough mass analysis with a resolving power of about 100. This is sufficient to distinguish between different cluster sizes. However, as Figure 8 shows for the example of Al_{70}^-, the resolving power of the quadrupolar centring of about 3000 is more than sufficient to distinguish pure Al_{70}^- clusters (at a mass of 70×27 u = 1890 u) from Al_{70}^-H, i.e. clusters possibly contaminated by attachment of just one single hydrogen atom.

4 Conclusion and outlook

The first observation of aluminium cluster dianions has been reported. Preliminary results obtained for dianion creation by electron attachment to clusters ranging from Al_{34}^- to Al_{80}^- have been presented. No dianions were observed for clusters containing less than 34 atoms. The preliminary data recorded for cluster sizes ranging between Al_{34}^- and Al_{44}^- indicates that the relative abundance of dianions as a function of cluster size increases significantly over a small size range, from Al_{37} to Al_{40}. The dianion yield was found to increase as a function of the trapping voltage, i.e. as a function of the energy of the stored secondary electrons. The attachment was observed to continue for reaction times above 20 s. Preliminary quadrupolar resonance measurements at a few selected cluster sizes suggest that the clusters are not contaminated. It is intended to further characterise Al_n^{2-} creation with particular focus on the observed dependences of dianion yield on the trapping potential and the reaction time in the electron-bath. The method will also be applied with the aim of producing trianions as already observed in the case of gold clusters [36]. Subsequently, collisional and photoexcitation experiments are planned for size and charge-state selected multiply negatively charged aluminium clusters.

Financial support from the DFG652 Collaborative Research Centre is gratefully acknowledged. The authors thank the Max Planck Institute for Plasma Physics, Greifswald, for its kind hospitality and support and Falk Ziegler and Martin Breitenfeldt for their help in taking some of the data.

References

1. Xi Li et al., Phys. Rev. Lett. **81**, 1909 (1998)
2. A.K. Ray et al., J. Phys.: Condens. Matter **9**, 2859 (1997)
3. M.F. Jarrold et al., J. Chem. Phys. **85**, 5373 (1986)
4. W. Begemann et al., Z. Phys. D **3**, 183 (1986)
5. L. Hanley et al., J. Chem. Phys. **87**, 260 (1987)
6. U. Ray et al., Chem. Phys. Lett. **159**, 221 (1989)
7. M.F. Jarrold et al., J. Phys. Chem. **97**, 1746 (1993)
8. E. Cottancin et al., Z. Phys. D **40**, 288 (1997)
9. G. Ganteför et al., Phys. Rev. A **37**, 2716 (1988)
10. K.J. Taylor et al., Chem. Phys. Lett. **152**, 347 (1988)
11. R. Hettich et al., J. Am. Chem. Soc. **111**, 8582 (1989)
12. G. Ganteför et al., Chem. Phys. Lett. **217**, 600 (1994)
13. C. Yannouleas et al., Eur. Phys. J. D **16**, 81 (2001)
14. A. Herlert et al., Int. J. Mass Spec. **229**, 19 (2003)
15. A. Lassesson et al., Eur. Phys. J. D **34**, 73 (2005)
16. S. Krückeberg et al., Eur. Phys. J. D **9**, 169 (1999)
17. K. Leiter et al., Int. J. Mass Spec. **68**, 341 (1986)
18. S. Schauer et al., Phys. Rev. Lett. **65**, 625 (1990)
19. X.-B. Wang et al., Phys. Rev. Lett. **83**, 3402 (1999)
20. C. Stoermer et al., Int. J. Mass Spec. **206**, 63 (2001)
21. L. Schweikhard et al., Phys. Scripta **T59**, 236 (1995)
22. St. Becker et al., Rev. Sci. Instrum. **66**, 4902 (1995)
23. L. Schweikhard et al., Eur. Phys. J. D **24**, 137 (2003)
24. H. Weidele et al., Z. Phys. D **20**, 411 (1991)
25. L.S. Brown et al., Rev. Mod. Phys. **58**, 233 (1986)
26. R.D. Knight et al., Int. J. Mass Spec. and Ion Phys. **51**, 127 (1983)
27. H. Schnatz et al., Nucl. Instr. Meth. A **251**, 17 (1986)
28. A. Herlert et al., Phys. Scripta **T80**, 200 (1999)
29. L. Schweikhard et al., Phil. Mag. B **79**, 1343 (1999)
30. J.D. Jackson, *Classical Electrodynamics*, 3rd edn. (Wiley and sons Inc, USA, 1998), pp. 57–62
31. `http://periodic.lanl.gov/elements/13.html`
32. L.-S. Wang et al., Phys. Rev. Lett. **81**, 2667 (1988)
33. O. Hampe et al., Chem. Phys. Lett. **354**, 303 (2002)
34. O. Ehrler et al., Phys. Rev. Lett. **91**, 113006 (2003)
35. B.H. Bransden et al. *Quantum Mechanics*, 2nd edn. (Pearson Education Ltd., 2000), pp. 408–426
36. C. Yannouleas et al., Phys. Rev. Lett. **86**, 2996 (2001)
37. L. Schweikhard et al., AIP Conf. Proc. **692**, 203 (2003)
38. G. Savard et al., Phys. Lett. A **158**, 247 (1991)
39. H.-U. Hasse et al., Int. J. Mass Spec. **132**, 181 (1994)